Nonlinear Dynamics of the $m=1$ Instability and Fast Sawtooth Collapse in High-Temperature Plasmas

Xiaogang Wang and A. Bhattacharjee
Department of Applied Physics, Columbia University, New York, New York 10027
(Received 3 November 1992)

A theory is given for the nonlinear dynamical evolution of the $m=1$ instability, governed by a generalized Ohm's law that includes the Hall term. An island equation is derived for the entire nonlinear evolution which includes an almost explosive growth phase followed by a rapid decay phase. The predictions of the theory are compared with recent numerical results and experiments.

PACS numbers: 52.35.Py, 52.55.Fa

In the seventies, essential features of the observed sawtooth collapse in tokamaks were accounted for by the Kadomtsev model [1]. Kadomtsev, who gave a heuristic theory for the nonlinear evolution of the $m=1$ kink-tearing instability, demonstrated that in the nonlinear phase, the instability causes reconnection at the $q=1$ rational surface on the characteristic Sweet-Parker time scale [2] $\tau_K=(\tau_A\tau_R)^{1/2}$, where τ_A is the Alfvén time scale and τ_R is the resistive diffusion time scale. For most tokamaks operating during the seventies, the time scales τ_A and τ_R were typically of the order of 10^{-7} s and 10^{-1} s, respectively, which gave $\tau_K\sim 100$ μs, in agreement with the sawtooth collapse time then observed.

In larger and hotter tokamaks such as JET [3] and TFTR [4], the Kadomtsev model predicts a time scale τ_K which is 1 to 2 orders of magnitude larger than the observed collapse time. (It is not uncommon in these devices to obtain collapse times $\tau_S\sim 20$–100 μs whereas $\tau_K\sim 2$–10 ms.) This discrepancy has stimulated considerable theoretical research, and at present it is widely believed that the nonlinear evolution of the $m=1$ mode in the collisionless (or semicollisional) regime that characterizes high-temperature plasmas can account for the fast sawtooth collapse. In recent calculations, instead of classical resistivity which provides the dissipation mechanism in resistive magnetohydrodynamics (MHD), one invokes other mechanisms such as electron inertia [5–7] or hyper-resistivity [7,8] or both [7]. While all of these calculations predict fast sawtooth crashes, they do not account for the time development of the growth rate, known otherwise as the "fast trigger problem" [9–11].

The fast trigger problem is concerned with the *onset* of the sawtooth collapse. The issue that remains essentially unresolved in the calculations cited above is the mechanism by which a sudden and spontaneous transition occurs from the sawtooth ramp phase to the collapse phase.

Aydemir [12] has recently reported nonlinear computational results based on the four-field, two-fluid equations of Hazeltine, Hsu, and Morrison [13]. These results, we believe, represent a significant step in developing a more complete understanding of sawtooth oscillations. One of the striking features of Aydemir's simulation is a strong nonlinear enhancement of the growth rate of the $m=1$ instability over its linear value [6,14–17]. This nonlinear enhancement occurs suddenly, indeed almost explosively, after which the growth rate decreases rapidly from its peak value to zero as the reconnection is completed. The geometry of the separatrix is reported to change from the Y points [18,19] that characterize a resistive MHD island to an X point, which leads to the fast reconnection observed in the simulation.

In this paper, we propose an analytical model which explains the salient features of Aydemir's simulation, and provides a solution of the fast trigger problem for sawtooth collapse. The generalized (collisionless) Ohm's law can be written as

$$\mathbf{E}+\frac{\mathbf{v}_e\times\mathbf{B}}{c}=\frac{m_e}{ne^2}\left(\frac{\partial}{\partial t}+\mathbf{v}_e\cdot\nabla\right)\mathbf{J}-\frac{\nabla p}{ne}, \tag{1}$$

where $\mathbf{E}$ is the electric field, $\mathbf{B}$ is the magnetic field, $\mathbf{v}_e$ is the electron flow velocity, $\mathbf{J}=(c/4\pi)\nabla\times\mathbf{B}$ is the plasma current, m_e is the electron mass, e is the electron charge, n is the electron number density, and p is the electron pressure. The last term on the right-hand side of Eq. (1) is the so-called Hall term, the effect of which on the nonlinear $m=1$ instability is the main focus of this paper. Though the Hall term cannot break field lines, it nevertheless has a profound influence on the dynamics of the instability because it introduces a new spatial scale, of the order of the ion gyroradius ρ_i, which is the spatial scale of the parallel electric field $E_\parallel$ near the singular layer. The spatial scale of $J_\parallel$ is much narrower, of the order of the skin depth $\delta\equiv c/\omega_{pe}$.

We write $\mathbf{B}=B_T\hat{\mathbf{z}}+\hat{\mathbf{z}}\times\nabla_\perp\psi$, where B_T is the (constant) toroidal field, $\hat{\mathbf{z}}$ is the unit vector in the toroidal direction, and ψ is the poloidal flux function. In the four-field model [13], the parallel component of (1) gives

$$\frac{1}{c}\frac{d\psi}{dt}\equiv\frac{1}{c}\frac{\partial\psi}{\partial t}+\nabla_\parallel\phi=\frac{m_e}{ne^2}\left(\frac{\partial j}{\partial t}+[\phi,j]\right)-\frac{\nabla_\parallel p}{ne}, \tag{2}$$

where $\nabla_\parallel f\equiv\partial f/\partial z+[\psi,f]/B_T$, $[f,g]\equiv\hat{\mathbf{z}}\cdot\nabla_\perp f\times\nabla_\perp g$, $\mathbf{v}=\hat{\mathbf{z}}\times\nabla\phi$, $\Phi=B_T\phi/c$ is the electrostatic potential, and

$j=(c/4\pi)\nabla_\perp^2\psi$. Since we are considering the nonlinear evolution of a single Fourier mode ($m=1$, $n=1$), it is convenient to introduce a helical angle $\theta-z/R$, where θ is the poloidal angle in the standard cylindrical coordinates (r,θ,z), and R is the major radius. We define the helical field $\mathbf{B}_*=\hat{\mathbf{z}}\times\nabla_\perp\psi_*$, where ψ_* is the helical flux function. Note that $B_{*\theta}=B_\theta(1-q)$ vanishes at the $q=rB_T/RB_\theta=1$ rational surface. We can write $\partial/\partial z=-R^{-1}\partial/\partial\theta=-(B_\theta/rB_T)\partial/\partial\theta$, and

$$\nabla_\parallel f=(B_{*\theta}/rB_T)\partial f/\partial\theta=B_T^{-1}\hat{\mathbf{z}}\cdot\nabla_\perp\psi_*\times\nabla_\perp f\equiv B_T^{-1}[\psi_*,f]\,.$$

With these definitions, the left-hand side of (2) can be written as $c^{-1}d\psi_*/dt$.

From flux conservation in the exterior region, we have $d\psi_*/dt=v_rB_{*\theta}$. It can be demonstrated that in the nonlinear phase of the instability, the Hall term $\nabla_\parallel p/ne$ gives the dominant contribution to the radial flow velocity at the spatial scale ρ_i near the singular layer. We denote by v_c the radial flow caused by the electron inertia term [5,20]. Then $|v_c|\sim(\delta/\rho_i)|v_r|$. Since $\rho_i\gg\delta$, we have $|v_c|\ll|v_r|$. Consequently, Ohm's law (2) gives [2,21]

$$\frac{v_rB_{*\theta}}{c}\simeq-\frac{\nabla_\parallel p}{ne}\simeq-\frac{B_{*\theta}}{B_Tr_sne}\frac{\partial p}{\partial\theta}\,, \tag{3}$$

where $r=r_s$ is the radial location of the $q=1$ surface.

From the continuity equation, we get [19]

$$v_0\Delta=\int_0^{\theta_0}v_rr_s\,d\theta'=u_0r_s\int_0^{\theta_0}\cos\theta'\,d\theta'=u_0r_s\sin\theta_0\,, \tag{4}$$

where Δ is the width of the current sheet, $\theta'=\pm\theta_0$ designate the poloidal locations of the two tips of the $m=1$, $n=1$ island [Fig. 1(a)], $v_0=v_\theta(\theta_0)$, $\theta'=\pi-\theta$, and $u_0=v_r(\theta'=0)$.

We now use the parallel component of the force balance condition along the sheet, which gives $\partial/\partial\theta(\rho v_\theta^2+p)=0$ [19]. Integrating (3), we obtain

$$\int_0^{\theta_0}v_r\,d\theta'=\frac{c}{ner_sB_T}\int_{\theta_0}^{0}\frac{\partial p}{\partial\theta}d\theta=\frac{c}{ner_sB_T}\int_0^{\theta_0}\frac{\partial}{\partial\theta}(\tfrac{1}{2}nm_iv_\theta^2)d\theta\,. \tag{5}$$

From (4) and (5), it follows that

$$u_0\sin\theta_0=v_0^2/2\Omega_ir_s\,, \tag{6}$$

where $\Omega_i\equiv eB_T/m_ic$ is the ion Larmor frequency. As shown by simple geometric considerations in Ref. [19], $u_0=\frac{1}{4}dw/dt$, where w is the width of the island and $v_0=B_{*\theta}/(4\pi nm_i)^{1/2}$. It can also be shown that $B_{*\theta}=|\psi_0''(r_s)|w/2\equiv B_pw/2r_s$ where $\psi_0''(r_s)=-B_\theta(r_s)q'(r_s)$ and $B_p\equiv|\psi_0''(r_s)|r_s$. From (4) and (6), we get

$$\Delta=v_0/2\Omega_i\,. \tag{7}$$

Defining $x\equiv w/2r_s$, $v_A\equiv B_p/(4\pi nm_i)^{1/2}$, $\omega_A\equiv v_A/r_s$, and $\gamma_0\equiv\omega_A^2/\Omega_i$, Eq. (6) yields

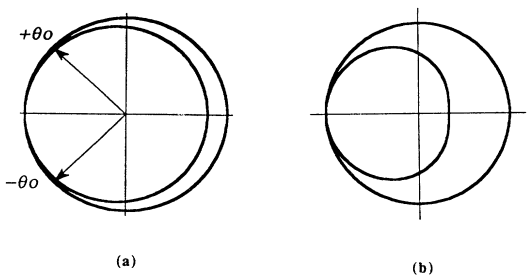

FIG. 1. (a) Schematic plot of Y points in the early stages of the nonlinear evolution of the instability. (b) Schematic plot of the X point that tends to form in the explosive phase of the instability. Note the distortion from circularity of the inner surface.

$$\frac{dx}{dt}\simeq\frac{\gamma_0}{\sin\theta_0}x^2\,. \tag{8}$$

We shall demonstrate later that $\sin\theta_0\simeq(\omega_A/\Omega_i)^{1/2}$. Equation (8) then implies that $x\sim1/(t_c-t)$, where t_c is a positive constant. As $t\to t_c$, an explosive growth of the island tends to occur. We propose that this fast blowup in time accounts for the sudden *onset* of the sawtooth crash. This fast blowup should be contrasted with the slow algebraic growth of a nonlinear resistive MHD island for which $w\sim t^2$ [18,19].

It should be noted that the finite-time singularity predicted by (8) is not realized in practice. This is because Eq. (8) relies on the thin-island approximation, $w/r_s\ll1$, which breaks down when the island size becomes a significant fraction of the plasma radius. Furthermore, this process is so strongly time dependent that it is not possible to treat the nonlinear evolution of the instability as a sequence of neighboring equilibria [18,22–24]. Rather remarkably, however, this evolution can be understood by introducing a simple correlation in the expression for ψ_*.

As in Ref. [22], we label flux surfaces by their radial position in the equilibrium configuration. If we define $x=r-r_s$, then the helical flux function can be labeled by $x_0=r_0-r_s$, where r_0 is the position of the unperturbed flux surface. We then have

$$\psi_*\simeq\tfrac{1}{2}\psi_0''x_0^2=\tfrac{1}{2}\psi_0''[x+\xi(x,\theta)]^2\,, \tag{9}$$

where $\xi(x,\theta)$ is the radial displacement of the flux surface from its initial position. We take $\xi(x,\theta)=\xi\cos\theta$ with $\xi=0$ for $x>0$, and $\xi=$const for $x<0$. In Fig. 1(a), the outer branch of the separatrix is given by $x_e=x_0(r_s+w/4)=w/4$. The inner branch is given by $x_i+\xi\cos\theta=x_0(r_s-w/4)=-w/4$, or $x_i=-w/4-\xi\cos\theta$. Then $w=2\xi$. An X point tends to form at the intersection of the inner and outer branches, with coordinates $x=w/4$, $\theta=\pi$. At this point, the exterior region solution exhibits a current singularity and a jump in the helical field given by $\Delta B_{*\theta}=\psi_0''[w/4-(-w/4)]$

$=\frac{1}{2}\psi_0''w$. The tendency for X-point formation is depicted schematically in Fig. 1(b), and is consistent with the numerical results reported by Aydemir (see Fig. 2 of Ref. [12]). Note also that the inner flux surface in Fig. 1(b) is deformed from its initially circular shape. This is indeed what is seen in Aydemir's simulation [12] as well as experiments [4].

The slowing down of the nearly explosive growth of the island occurs due to the reduction in the magnitude of $B_{*\theta}$ from the value $B_{*\theta}=B_p w/2r_s$. This reduction can be calculated from the relation [22]

$$B_{*\theta}=\frac{\partial\psi_*}{\partial r}=\frac{\partial\psi_0}{\partial r}\bigg|_{r-\xi}, \tag{10}$$

where ψ_0 is the flux function in the initial cylindrical equilibrium. Expanding the right-hand term in (10), we get

$$B_{*\theta}\simeq\frac{|\psi_0''|}{r_s}\xi(r_s-\xi)=B_p\frac{w}{2r_s}\left(1-\frac{w}{2r_s}\right). \tag{11}$$

The distance between the inner and outer surfaces bounding the island is given by

$$d(\theta)=\frac{w}{4}-\left(-\frac{w}{4}-\xi\cos\theta\right)=w\sin^2\frac{\theta}{2}. \tag{12}$$

If $\Delta<d$, a thin sheet current encompassing two distinct Y points at $\theta'=\pi-\theta=\pm\theta_0$ persists, where θ_0 is determined by the relation $d(\theta_0)=\Delta$. This relation gives $\Delta=w\sin^2\theta_0/2$. Since, by (7), $\Delta=(\omega_A/4\Omega_i)w$, and typically $\Omega_i\gg\omega_A$, we have

$$\sin\theta_0=2\sin\frac{\theta_0}{2}\cos\frac{\theta_0}{2}=\left(\frac{\omega_A}{\Omega_i}\right)^{1/2}\left(1-\frac{\omega_A}{4\Omega_i}\right)^{1/2}\simeq\left(\frac{\omega_A}{\Omega_i}\right)^{1/2}, \tag{13}$$

as asserted earlier. We now demonstrate that even as the angle θ_0 becomes small due to the effect of the Hall term, the current sheet is still characterized by the property that its (poloidal) length L is much larger than its (radial) width Δ, as in the Sweet-Parker model [2]. To see this, we note that $L=2r_s\theta_0$ and $\Delta=W\sin^2(\theta_0/2)$. (For a resistive MHD island, $\theta_0\simeq\pi/3$ and $W\ll r_s$ [18,19]; hence $\Delta\ll L$.) For very small values of θ_0, since $\Delta\simeq W\theta_0^2/4$, $\Delta/L\simeq W\theta_0/8r_s$, and $W\leq r_s$, the smallness of θ_0 implies that $\Delta\ll L$. Thus, what is realized in the simulation discussed in Ref. [12] cannot be called, strictly speaking, an X point. Rather, what occurs is that the strip connecting the two Y points shrinks drastically as the island width increases.

For thin islands, Eq. (8) gives

$$\frac{dx}{dt}\simeq\left(\frac{\omega_A}{\Omega_i}\right)^{1/2}\omega_A x^2\equiv\Gamma_0 x^2, \tag{14}$$

which yields $x=1/\Gamma_0(t_c-t)$ with $t_c=2r_s/\Gamma_0 w(t_0)$, where $t=t_0$ denotes the time of onset of the nonlinear phase which follows the linear phase. In order to estimate $w(t_0)$, we note that in the simulation of Ref. [12] there is little deviation from the linear growth rate γ_L in the early nonlinear phase of the instability. We, therefore, set $\gamma(t_0)\sim\gamma_L\sim0.5\omega_A(\delta/r_s)(\rho_i/\delta)^{2/3}$ [6,14]. (Note that the multiplicative factor 0.5 in γ_L is necessary because we are considering here the growth of the island which grows half as fast as the perturbed magnetic field.) For JET, with $B_T=3$ T, $n_i=3\times10^{19}/\mathrm{m}^3$, $R=3$ m, we have $\omega_A\simeq(v_A/R)q'r_s\simeq4\times10^6$/s, $\Gamma_0\sim10^6$/s, and consequently $\gamma(t_0)\sim\Gamma_0 x(t_0)=0.1\omega_A w(t_0)/r_s$. This, in turn, means that $w(t_0)\sim0.9$ cm since $\delta\sim0.1$ cm and $\rho_i\sim0.3$ cm. Taking $r_s=0.3$ m, we obtain $t_c\sim70$ μs.

An equation for the entire nonlinear evolution of the island can be obtained using Eqs. (6), (11), and (12). We get

$$\frac{dx}{d\tau}\sim2x^2(1-x)^{3/2}\left(\frac{4}{\gamma_0}-1+x\right)^{-1/2}, \tag{15}$$

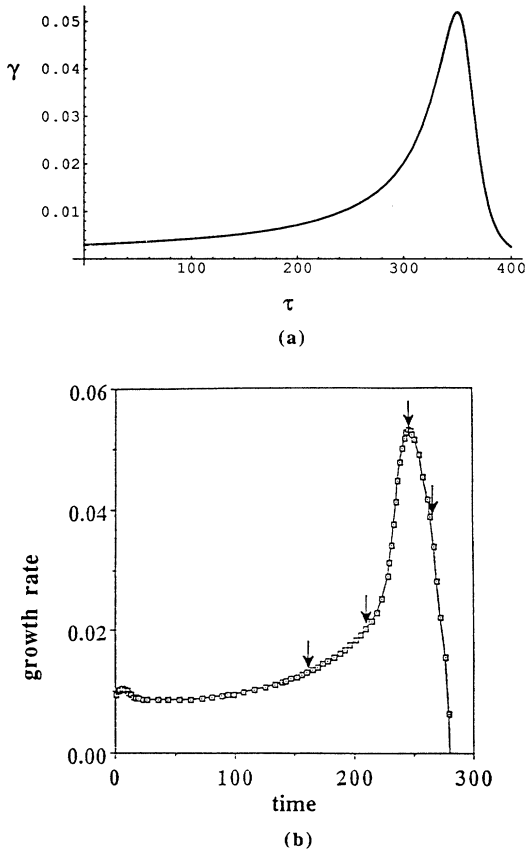

FIG. 2. (a) The nonlinear growth rate for the island width predicted by theory. (b) The nonlinear growth rate obtained numerically in Ref. [12]. The physical parameters and initial conditions for this calculation are somewhat different from those used for (a).

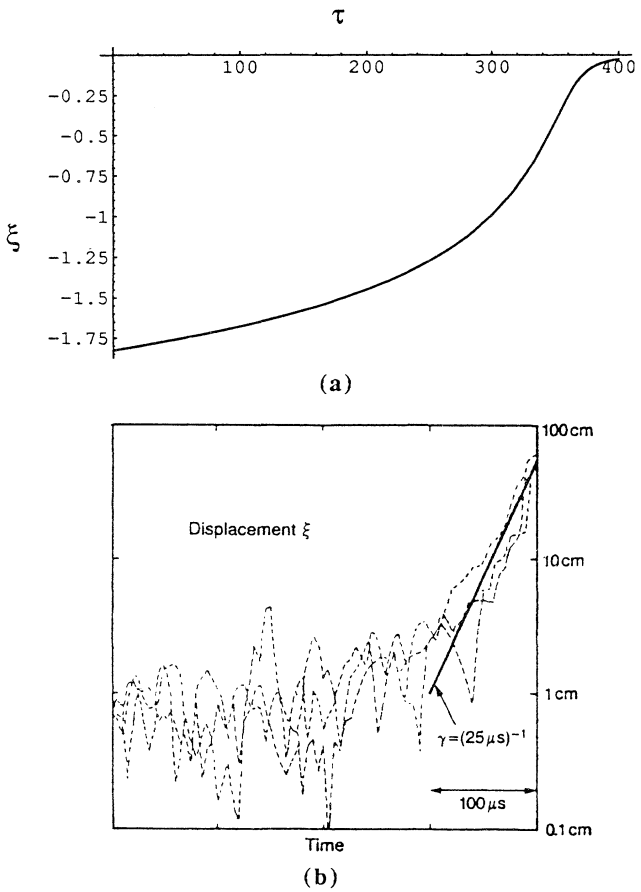

FIG. 3. (a) The displacement of the plasma predicted by theory. (b) The displacement as inferred from the peak soft-x-ray emissivity in the JET device reported in Ref. [11].

where $\tau \equiv \omega_A t$ and γ_0 has been normalized by ω_A. We define the nonlinear growth rate

$$\gamma = \frac{d}{d\tau} \ln w \simeq 2x(1-x)^{3/2} \left[\frac{4}{\gamma_0} - 1 + x \right]^{-1/2} . \quad (16)$$

Equation (13) is integrated with the initial condition $w(t_0) = \rho_i$ and the JET parameters cited earlier. The nonlinear growth rate γ is plotted in Fig. 2(a). [For convenience, we have chosen $t_0 = 0$ in Fig. 2(a).] Figure 2(b) is the analogous plot given by Aydemir [12]. We emphasize only the *qualitative* similarity between Figs. 2(a) and 2(b); the two plots do not correspond to identical physical parameters or initial conditions, and show some quantitative differences.

Figure 3(a) is a logarithmic plot of the displacement ξ versus time which resembles closely the plot of the peak soft-x-ray emission for three sawtooth collapses, reported in Ref. [11], and reproduced here as Fig. 3(b). The value of γ^{-1} obtained from the slope of the plot in Fig. 3(a) during the final stages of the near-explosive growth is approximately 15 μs which compares well with the experimentally observed value of 25 μs. We remark here that the time scale of a sawtooth collapse depends on ω_A which in turn depends on the local magnetic shear. Some of the extreme sensitivity of the observed sawtooth time scales to the current profile, seen, for instance, in TFTR [4], may be attributed to the variation in the local magnetic shear at the $q = 1$ surface.

This research is supported by the U.S. Department of Energy Grant No. DE-FG02-92ER54168.

[1] B. B. Kadomtsev, Fiz. Plasmy **1**, 710 (1975) [Sov. J. Plasma Phys. **1**, 389 (1975)]. This model was also independently discovered by D. A. Monticello (unpublished).
[2] P. A. Sweet, in *Electromagnetic Phenomena in Cosmical Physics*, edited by B. Lehnert (Cambridge Univ. Press, New York, 1958), p. 123; E. N. Parker, J. Geophys. Res. **62**, 509 (1957).
[3] D. J. Campbell and the JET Group, Phys. Rev. Lett. **57**, 210 (1986).
[4] K. McGuire and the TFTR Group, Phys. Fluids B **2**, 1287 (1990).
[5] J. A. Wesson, Nucl. Fusion **30**, 2545 (1990).
[6] F. Porcelli, Phys. Rev. Lett. **66**, 425 (1991).
[7] J. F. Drake and R. G. Kleva, Phys. Rev. Lett. **66**, 1458 (1991).
[8] A. Y. Aydemir, Phys. Fluids B **2**, 2135 (1990).
[9] J. A. Wesson, P. Kirby, and M. F. Nave, in *Plasma Physics and Controlled Nuclear Fusion Research 1986* (IAEA, Vienna, 1987), Vol. 2, p. 3.
[10] A. Y. Aydemir, J. C. Wiley, and D. W. Ross, Phys. Fluids B **1**, 779 (1989).
[11] J. A. Wesson, A. W. Edwards, and R. S. Granetz, Nucl. Fusion **31**, 111 (1991).
[12] A. Y. Aydemir, Phys. Fluids B **4**, 3469 (1992).
[13] R. D. Hazeltine, C. T. Hsu, and P. J. Morrison, Phys. Fluids **30**, 3204 (1987).
[14] J. F. Drake, Phys. Fluids **21**, 1777 (1978).
[15] H. L. Berk, S. M. Mahajan, and Y. Z. Zhang, Phys. Fluids B **3**, 351 (1991).
[16] A. Y. Aydemir, Phys. Fluids B **3**, 3025 (1991).
[17] L. Zakharov and B. Rogers, Phys. Fluids B **4**, 3285 (1992).
[18] F. L. Waelbroeck, Phys. Fluids B **1**, 2372 (1989).
[19] D. Biskamp, Phys. Fluids B **3**, 3353 (1991).
[20] B. Basu and B. Coppi, Phys. Fluids **24**, 465 (1981).
[21] W. Park, D. A. Monticello, and R. B. White, Phys. Fluids **27**, 137 (1984).
[22] M. N. Rosenbluth, R. Y. Dagazian, and P. H. Rutherford, Phys. Fluids **16**, 1894 (1973).
[23] K. Avinash, R. J. Hastie, J. B. Taylor, and S. C. Cowley, Phys. Rev. Lett. **59**, 2647 (1987).
[24] M. N. Bussac and R. Pellat, Phys. Rev. Lett. **59**, 2650 (1987).